

On the existence of Ulanowicz's optimal structural resilience in complex networks

Si-Yao Wei^{a,b}, Wei-Xing Zhou^{a,b,c,*}

^a*School of Business, East China University of Science and Technology, Shanghai 200237, China*

^b*Research Center for Econophysics, East China University of Science and Technology, Shanghai 200237, China*

^c*School of Mathematics, East China University of Science and Technology, Shanghai 200237, China*

Abstract

This study investigates the mathematical existence and asymptotic properties of Ulanowicz's structural resilience in complex systems such as supply chain networks. While ecological evidence suggests that sustainable systems gravitate toward an optimal state at $\alpha = 1/e$, the universality of this configuration in generalized networks remains theoretically unverified. We prove that while optimal resilience is unattainable in two-node networks due to structural over-determinacy, it exists for any directed graph with $N_V \geq 3$. By constructing a symmetric network model with three types of link weights (x, y, z) and uniform marginal distributions, we derive the governing equations for the optimal resilience configuration. Our analytical and numerical results reveal that as the network size N_V increases, the link weights required to maintain optimal resilience exhibit a power-law scaling behavior: the adjacent links scale as $O(N_V^{-1})$, while the non-adjacent links scale as $O(N_V^{-2})$, both accompanied by specific logarithmic corrections. This work establishes a rigorous mathematical foundation for the optimal resilience framework and provides a unified perspective on how entropy-based principles govern the robustness and evolution of large-scale complex networks, which may offer quantitative guidance for designing large-scale networked systems under robustness constraints.

Keywords: Complex networks; Structural resilience; Power-law scaling; Asymptotic behaviour

*Corresponding author.

Email address: wxzhou@ecust.edu.cn (Wei-Xing Zhou)

1. Introduction

Resilience is a fundamental property of complex systems (Liu et al., 2022) and thereby, that in complex networks has emerged as a focal point of interdisciplinary research, spanning from ecological stability (Seidl et al., 2016) and infrastructure reliability (Chen et al., 2024) to the robustness of global economic systems (Brunnermeier, 2024) and supply chains (Ivanov, 2024; Cohen et al., 2022). Various studies suggest that modern complex systems must simultaneously achieve high operational efficiency and sufficient redundancy to withstand disruptions (Lücker et al., 2025; Kahiluoto et al., 2020; Yang et al., 2024). However, these two objectives are often conflicting: highly optimized networks tend to be fragile, whereas overly redundant systems incur excessive operational costs. Understanding and quantifying this trade-off has therefore become a fundamental research challenge in network optimization and robust system design (Pettit et al., 2019; Zhu et al., 2025).

Entropy-based performance measures have recently attracted increasing attention as tools for characterizing structural robustness in complex networks. In the field of theoretical ecology, Ulanowicz (1979) proposed an information-theoretic framework to quantify this tension, defining system fitness or structural resilience as a function of the balance between efficiency and redundancy (Ulanowicz and Norden, 1990; Ulanowicz, 2009). Within this framework, efficiency is associated with the mutual information of the flow distribution, while redundancy corresponds to the conditional entropy (or overhead). Central to this theory is the “Window of Vitality” hypothesis, which suggests that sustainable and resilient ecosystems do not maximize efficiency or redundancy. Instead, they gravitate toward an optimal configuration where the degree of order, denoted by α , is approximately $1/e \approx 0.3679$. At this critical point, the system is argued to possess sufficient articulation to function effectively and enough diversity to adapt to changing environments.

Despite the empirical success of Ulanowicz’s metrics in describing biological food webs (Ulanowicz, 2009), industrial metabolic networks (Liang et al., 2020), and international trade networks (Kharrazi et al., 2013), several theoretical questions remain unanswered. First, is the existence of an optimal resilience configuration a unique hallmark of biological selection, or is it a univer-

sal structural property inherent to any sufficiently complex directed network? Second, how does the network size and the underlying topology constrain the possibility of reaching this optimum? Existing studies often focus on specific, data-driven instances, leaving a gap in the rigorous mathematical understanding of these entropy-based measures in generalized network configurations.

In this paper, we investigate the mathematical existence and asymptotic behavior of Ulanowicz's optimal resilience in complex networks. We begin by demonstrating that for small-scale systems, such as two-node networks, the optimal resilience $R = 1/e$ is unattainable due to structural over-determinacy. However, as we move to networks with $N_V \geq 3$, we prove the existence of at least one flow configuration that satisfies the optimality condition. By constructing a symmetric network model with three types of link weights, we derive governing equations for optimal resilience and analyze their solutions as N_V tends to infinity. Our results reveal a scaling behavior: the link weights required to maintain optimal resilience follow a power-law distribution with respect to the network size, accompanied by specific logarithmic corrections.

This study provides a unified theoretical framework for understanding how entropy optimization governs robustness across different scales. The remainder of this paper is organized as follows: Section 2 formalizes the definitions of efficiency, redundancy, and structural resilience. Section 3 presents the analysis of the general N_V -node symmetric model, including the proofs of the existence theorems and asymptotic scaling laws. Finally, Section 4 discusses the implications of these findings for the design and control of robust complex systems.

2. Definitions

2.1. Efficiency and redundancy

Consider a weighted digraph $G = \langle \mathcal{V}, \mathcal{E} \rangle$, where \mathcal{V} represents the vertex set with N_V vertices and \mathcal{E} represents the link set with N_E links. Let f_{ij} denote the flow from vertex i to vertex j . The out-strength of vertex i is $s_i^{\text{out}} = \sum_{j=1}^{N_V} f_{ij}$ and the in-strength of vertex j is $s_j^{\text{in}} = \sum_{i=1}^{N_V} f_{ij}$. The throughput $s = \sum_{i=1}^{N_V} s_i^{\text{out}} = \sum_{j=1}^{N_V} s_j^{\text{in}} = \sum_{i=1}^{N_V} \sum_{j=1}^{N_V} f_{ij}$.

In information theory, entropy measures a system's uncertainty (or diversity). A higher entropy reflects greater unpredictability and diversity, indicating an enhanced adaptability to chang-

ing conditions and an improved capacity of the system to absorb shocks (Khakifirooz et al., 2025; Reggiani, 2022). Accordingly, we can adopt joint entropy to characterize a system's overall structural properties (Rutledge et al., 1976; Ulanowicz, 1979), which is also called as “capacity” for system development (Ulanowicz and Norden, 1990):

$$H = - \sum_{i=1}^{N_V} \sum_{j=1}^{N_V} p_{ij} \ln p_{ij}. \quad (1)$$

Given that joint entropy is equal to the sum of mutual information and conditional entropy, we further introduce two underlying quantities, efficiency and redundancy, which demonstrate opposing properties of a system. Efficiency embodies the flow articulation within networked configurations, which tends to increase due to preferential interactions between nodes (Kharrazi et al., 2017). In information theory, a higher mutual information indicates a increased reduction in uncertainty when some information is known and a stronger statistical inter-dependence between variables. Hence, we define the efficiency e of digraph G as follows:

$$e = \sum_{i=1}^{N_V} \sum_{j=1}^{N_V} p_{ij} \ln \frac{p_{ij}}{p_i^{\text{out}} p_j^{\text{in}}} = \sum_{i=1}^{N_V} \sum_{j=1}^{N_V} \frac{f_{ij}}{s} \ln \frac{f_{ij}s}{s_i^{\text{out}} s_j^{\text{in}}}, \quad (2)$$

where

$$p_{ij} = \frac{f_{ij}}{s}, \quad p_i^{\text{out}} = \frac{s_i^{\text{out}}}{s}, \quad p_j^{\text{in}} = \frac{s_j^{\text{in}}}{s}. \quad (3)$$

Redundancy embodies the diversity of pathways, which is critical for a system's capacity adapting to changing environmental conditions arising from shocks or disturbances (Luo et al., 2024). Note that our perspective departs from studies that focus primarily on overall uncertainty and instead emphasizes the trade-off between efficiency and redundancy. In this context, redundancy is conceptualized as the residual uncertainty conditional on partial information, which corresponds to the definition of conditional entropy in information theory. A higher conditional entropy indicates a greater availability of alternative pathways and a consequently higher system

redundancy. Hence, the redundancy r of digraph G can be defined as

$$r = - \sum_{i=1}^{N_V} \sum_{j=1}^{N_V} p_{ij} \ln \frac{p_{ij}}{p_i^{\text{out}}} - \sum_{i=1}^{N_V} \sum_{j=1}^{N_V} p_{ij} \ln \frac{p_{ij}}{p_j^{\text{in}}} = \sum_{i=1}^{N_V} \sum_{j=1}^{N_V} \frac{f_{ij}}{s} \ln \frac{s_i^{\text{out}} s_j^{\text{in}}}{f_{ij}^2}. \quad (4)$$

2.2. Ulanowicz's structural resilience

Based on these two system properties, the ratio α , a more comprehensive metric to indicate the order of a system, is proposed for reflecting the trade-off between efficiency and redundancy (Goerner et al., 2009; Ulanowicz et al., 2009; Ulanowicz, 1979), expressed as

$$\alpha = \frac{e}{H} = \frac{e}{e + r}, \quad (5)$$

where $0 \leq \alpha \leq 1$.

Inspired by ecological systems, whose order parameters are often observed to be close to $1/e$ (Zorach and Ulanowicz, 2003), Ulanowicz (2009) defined the fitness F of a system for change to be the product of α and the Boltzmann measure of its disorder such that $F = -c\alpha \ln \alpha$, where c is an appropriate scalar constant and e is Euler's number. At $\alpha = 1/e$, the first derivative $F' = 0$, indicating that the system's fitness is maximized (or optimized). The underlying assumption is that ecosystems exhibit superior trade-off because they have undergone long-term natural selection (Ulanowicz, 2009; Liang et al., 2020; Kharrazi et al., 2013). Finally, let $c = 1$, the resilience R of G can be defined as

$$R = -\alpha \ln \alpha, \quad (6)$$

with the function shown in Fig. 1. When $\alpha > 1/e$, the system is more efficient and productive but more vulnerable, and vice versa it is more redundant but more inefficient. R vanishes when $\alpha = 0$ (overly redundant) or $\alpha = 1$ (overly efficient).

2.3. An example: Two-node networks

Consider a directed graph G with two vertices. Let $p_{12} = p$ and $p_{21} = 1 - p$, with $p_{11} = 0$ and $p_{22} = 0$. Also, we have $p_1^{\text{out}} = p_2^{\text{in}} = p_{12} = p$ and $p_2^{\text{out}} = p_1^{\text{in}} = p_{21} = 1 - p$. Substituting them into

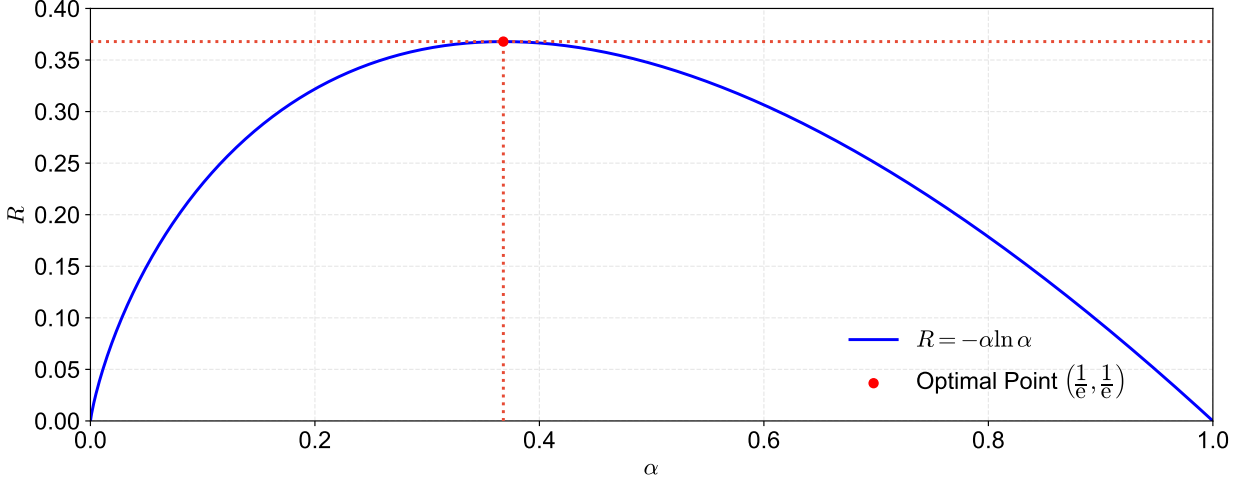


Fig. 1. The function $R = -\alpha \ln \alpha$.

Eq. (2) yields

$$\begin{aligned}
 e(p) &= \sum_{i=1}^2 \sum_{j=1}^2 p_{ij} \ln \frac{p_{ij}}{p_i^{\text{out}} p_j^{\text{in}}} \\
 &= -p \ln p - (1-p) \ln(1-p).
 \end{aligned} \tag{7}$$

According to Eq. (4), we have

$$\begin{aligned}
 r(p) &= - \sum_{i=1}^2 \sum_{j=1}^2 p_{ij} \ln \frac{p_{ij}}{p_i^{\text{out}}} - \sum_{i=1}^2 \sum_{j=1}^2 p_{ij} \ln \frac{p_{ij}}{p_j^{\text{in}}} \\
 &= 0.
 \end{aligned} \tag{8}$$

Accordingly, the ratio

$$\alpha(p) = \frac{e(p)}{e(p) + r(p)} \equiv 1 \quad \text{for } p \in [0, 1], \tag{9}$$

and the resilience

$$R(p) = -\alpha(p) \ln \alpha(p) = -1 \cdot \ln(1) = 0, \tag{10}$$

which represents that a two-vertex system with no self-loops is deterministic and overly-efficient. In other words, the optimal resilience ($R = 1/e$) does not exist in two-node networks.

3. Results

3.1. Governing equations

For a directed graph with N_V nodes and no self-loops ($p_{ii} = 0$ for all i), the joint probability matrix p_{ij} is defined based on the given conditions. The matrix is an $N_V \times N_V$ matrix where the elements are arranged as follows: (1) The elements immediately above the diagonal (in a circular sense) are x , i.e., $p_{i,i+1} = x$ for $i = 1, \dots, N_V - 1$, and $p_{N_V,1} = x$; (2) The elements immediately below the diagonal (in a circular sense) are y , i.e., $p_{i+1,i} = y$ for $i = 1, \dots, N_V - 1$, and $p_{1,N_V} = y$; and (3) All other off-diagonal elements are z . In other words, we have

$$p_{ij} = \begin{cases} x, & \text{if } j \equiv i + 1 \pmod{N_V} \text{ (forward cycle),} \\ y, & \text{if } j \equiv i - 1 \pmod{N_V} \text{ (backward cycle),} \\ z, & \text{otherwise, for } i \neq j \text{ (off-diagonal),} \\ 0, & \text{if } i = j \text{ (diagonal).} \end{cases} \quad (11)$$

The matrix can be represented as

$$\{p_{ij}\} = \begin{pmatrix} 0 & x & z & \cdots & z & y \\ y & 0 & x & \cdots & z & z \\ z & y & 0 & \cdots & z & z \\ \vdots & \vdots & \vdots & \ddots & \vdots & \vdots \\ z & z & z & \cdots & 0 & x \\ x & z & z & \cdots & y & 0 \end{pmatrix}. \quad (12)$$

A schematic representation of this network structure is shown in Fig. 2.

The probability normalization condition ensures that the sum of all probabilities is 1. The number of x elements is N_V , the number of y elements is N_V , and the number of z elements is $N_V(N_V - 3)$. Thus, the probability normalization equation is

$$N_Vx + N_Vy + N_V(N_V - 3)z = 1. \quad (13)$$

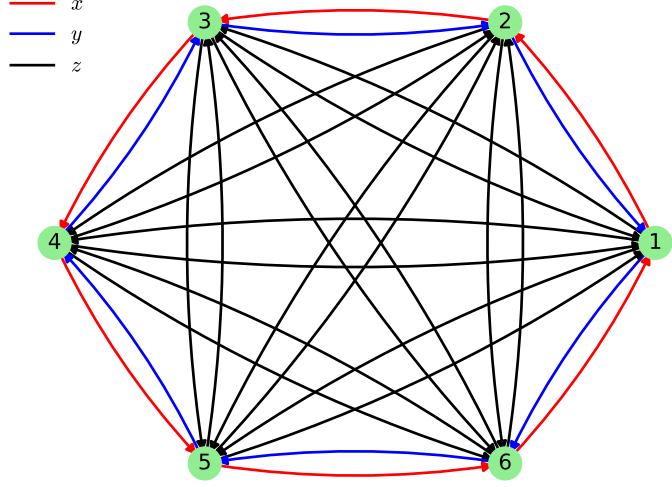


Fig. 2. The network represented by Eq. (11).

Simplifying, we get

$$x + y + (N_V - 3)z = \frac{1}{N_V}. \quad (14)$$

Due to symmetry, all nodes have identical marginals:

$$p_i^{\text{out}} = p_j^{\text{in}} = x + y + (N_V - 3)z = \frac{1}{N_V}, \quad (15)$$

which is the same as the probability normalization condition.

Accordingly, we have

$$e = \sum_{i=1}^{N_V} \sum_{j=1}^{N_V} p_{ij} \ln \frac{p_{ij}}{p_i^{\text{out}} p_j^{\text{in}}} = \sum_{i=1}^{N_V} \sum_{j=1}^{N_V} p_{ij} \ln p_{ij} + 2 \ln N_V, \quad (16)$$

where

$$\sum_{i=1}^{N_V} \sum_{j=1}^{N_V} p_{ij} \ln p_{ij} = N_V[x \ln x + y \ln y + (N_V - 3)z \ln z]. \quad (17)$$

Therefore, the efficiency e can be expressed as

$$e = N_V[x \ln x + y \ln y + (N_V - 3)z \ln z] + 2 \ln N_V. \quad (18)$$

For redundancy r , we have

$$r = 2 \ln N_V - 2e = -2N_V[x \ln x + y \ln y + (N_V - 3)z \ln z] - 2 \ln N_V. \quad (19)$$

Hence, we have

$$\begin{aligned} \alpha &= \frac{e}{2 \ln N_V - e} \\ &= -\frac{2 \ln N_V}{N_V[x \ln x + y \ln y + (N_V - 3)z \ln z]} - 1. \end{aligned} \quad (20)$$

The resilience R is maximized when $\alpha = 1/e$, which occurs when

$$e = \frac{2 \ln N_V}{e + 1}. \quad (21)$$

Furthermore, we have

$$x \ln x + y \ln y + (N_V - 3)z \ln z = -\frac{2e}{e + 1} \cdot \frac{\ln N_V}{N_V}. \quad (22)$$

Finally, we obtain the following equations:

$$\begin{cases} x + y + (N_V - 3)z = \frac{1}{N_V}, \\ x \ln x + y \ln y + (N_V - 3)z \ln z = -\frac{2e}{e + 1} \cdot \frac{\ln N_V}{N_V}, \end{cases} \quad (23)$$

where $x, y, z \geq 0$. Subsequently, we consider four cases, as presented in Fig. 3.

3.2. The case of $x = y$

3.2.1. Existence of solutions

Assume $x = y$. Then Eqs. (23) reduce to

$$\begin{cases} 2x + (N_V - 3)z = \frac{1}{N_V}, \\ 2x \ln x + (N_V - 3)z \ln z = -\frac{2e}{e + 1} \cdot \frac{\ln N_V}{N_V}, \end{cases} \quad (24)$$

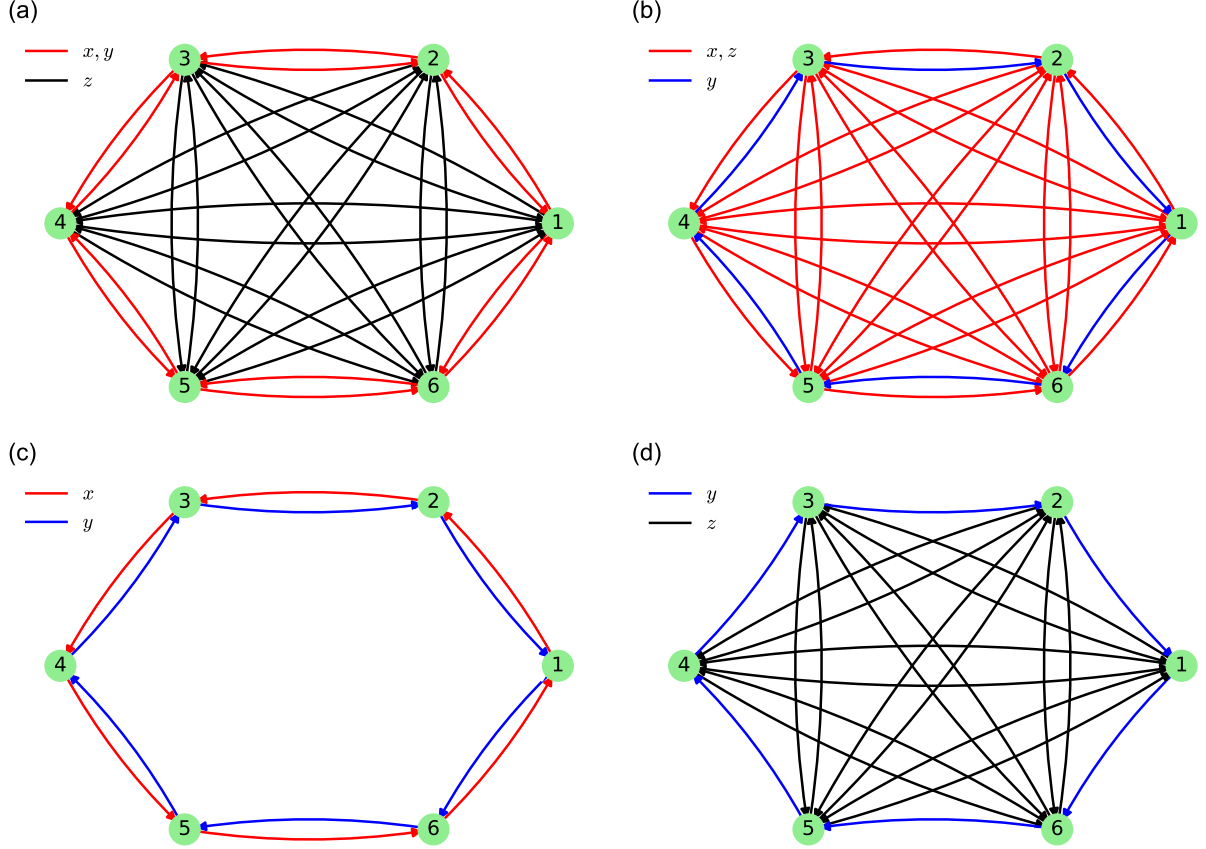


Fig. 3. Four cases of governing equations. (a) $x = y$, (b) $x = z$, (c) $z = 0$, and (d) $x = 0$.

where $x, z \geq 0$. The normalization condition yields

$$x = \frac{1}{2N_V} - \frac{(N_V - 3)z}{2}. \quad (25)$$

Substituting this expression into the second equation gives

$$2 \left[\frac{1}{2N_V} - \frac{(N_V - 3)z}{2} \right] \ln \left[\frac{1}{2N_V} - \frac{(N_V - 3)z}{2} \right] + (N_V - 3)z \ln z = -\frac{2e}{e + 1} \cdot \frac{\ln N_V}{N_V}. \quad (26)$$

The feasibility condition requires

$$0 \leq z \leq \frac{1}{N_V(N_V - 3)}. \quad (27)$$

To analyze the solution properties of Eq. (26), define

$$f(z) = 2 \left[\frac{1}{2N_V} - \frac{(N_V - 3)z}{2} \right] \ln \left[\frac{1}{2N_V} - \frac{(N_V - 3)z}{2} \right] + (N_V - 3)z \ln z + \frac{2e}{e + 1} \cdot \frac{\ln N_V}{N_V}. \quad (28)$$

Let $a = N_V - 3$ (with $a > 0$) and define

$$u(z) = \frac{1}{2N_V} - \frac{(N_V - 3)z}{2}. \quad (29)$$

Then

$$f(z) = 2u(z) \ln u(z) + az \ln z + \frac{2e}{e + 1} \cdot \frac{\ln N_V}{N_V}. \quad (30)$$

The first derivative of $f(z)$ is

$$\begin{aligned} f'(z) &= 2 \left[u'(z) \ln u(z) + u(z) \cdot \frac{u'(z)}{u(z)} \right] + a \left[\ln z + z \cdot \frac{1}{z} \right] \\ &= 2 [u'(z) \ln u(z) + u'(z)] + a(\ln z + 1) \\ &= 2u'(z)(\ln u(z) + 1) + a(\ln z + 1) \\ &= a \ln \left(\frac{z}{u(z)} \right). \end{aligned} \quad (31)$$

Hence, $f(z)$ is monotonically decreasing when $0 < z < \frac{1}{N_V(N_V - 1)}$ and monotonically increasing function when $\frac{1}{N_V(N_V - 1)} < z < \frac{1}{N_V(N_V - 3)}$. The minimum value is attained at

$$z = \frac{1}{N_V(N_V - 1)}, \quad (32)$$

with

$$f(z)_{\min} = f \left(\frac{1}{N_V(N_V - 1)} \right) = \frac{1}{N_V} \left(\frac{e - 1}{e + 1} \ln N_V - \ln(N_V - 1) \right). \quad (33)$$

For $N_V > 3$, $f(z)_{\min} < 0$.

The second derivative is

$$f''(z) = a \cdot \frac{d}{dz} [\ln z - \ln u(z)] = \frac{a}{z} + \frac{a^2}{2u(z)}, \quad (34)$$

which is non-negative on the feasible domain, indicating that $f(z)$ is convex.

At the boundary points, we have

$$f(0) = -\frac{1}{N_V} \ln(2N_V) + \frac{2e}{e+1} \cdot \frac{\ln N_V}{N_V} \quad (35)$$

and

$$f\left(\frac{1}{N_V(N_V-3)}\right) = -\frac{1}{N_V} \ln(N_V(N_V-3)) + \frac{2e}{e+1} \cdot \frac{\ln N_V}{N_V}. \quad (36)$$

Combining the convexity of $f(z)$ and the boundary values, we conclude that: (1) when $N_V = 4$, we have $f(0) < 0$ and $f\left(\frac{1}{N_V(N_V-3)}\right) > 0$, thus Eq. (26) has a unique solution; (2) when $N_V = 5$, we have $f(0) > 0$ and $f\left(\frac{1}{N_V(N_V-3)}\right) > 0$, thus Eq. (26) has two solutions; and (3) when $N_V \geq 6$, we have $f(0) > 0$ and $f\left(\frac{1}{N_V(N_V-3)}\right) < 0$, thus Eq. (26) has a unique solution. The above situations are illustrated in Fig. 4(a), which reveals the existence of solutions of the optimal resilience when $x = y$.

3.2.2. Asymptotic behavior of solutions

Furthermore, by numerically solving $f(z) = 0$ for increasing N_V , we observe that when N_V becomes sufficiently large (e.g., $N_V > 10^2$), the relationship between N_V and the corresponding root z forms an approximately straight line in the double-logarithmic coordinate system, which suggests a power-law scaling. To describe the asymptotic behavior of the root pair (x, z) for large network size N_V , we introduce scaled variables

$$A = 2N_V x, \quad B = (N_V - 3)N_V z, \quad (37)$$

such that Eq. (25) is equivalent to

$$A + B = 1. \quad (38)$$

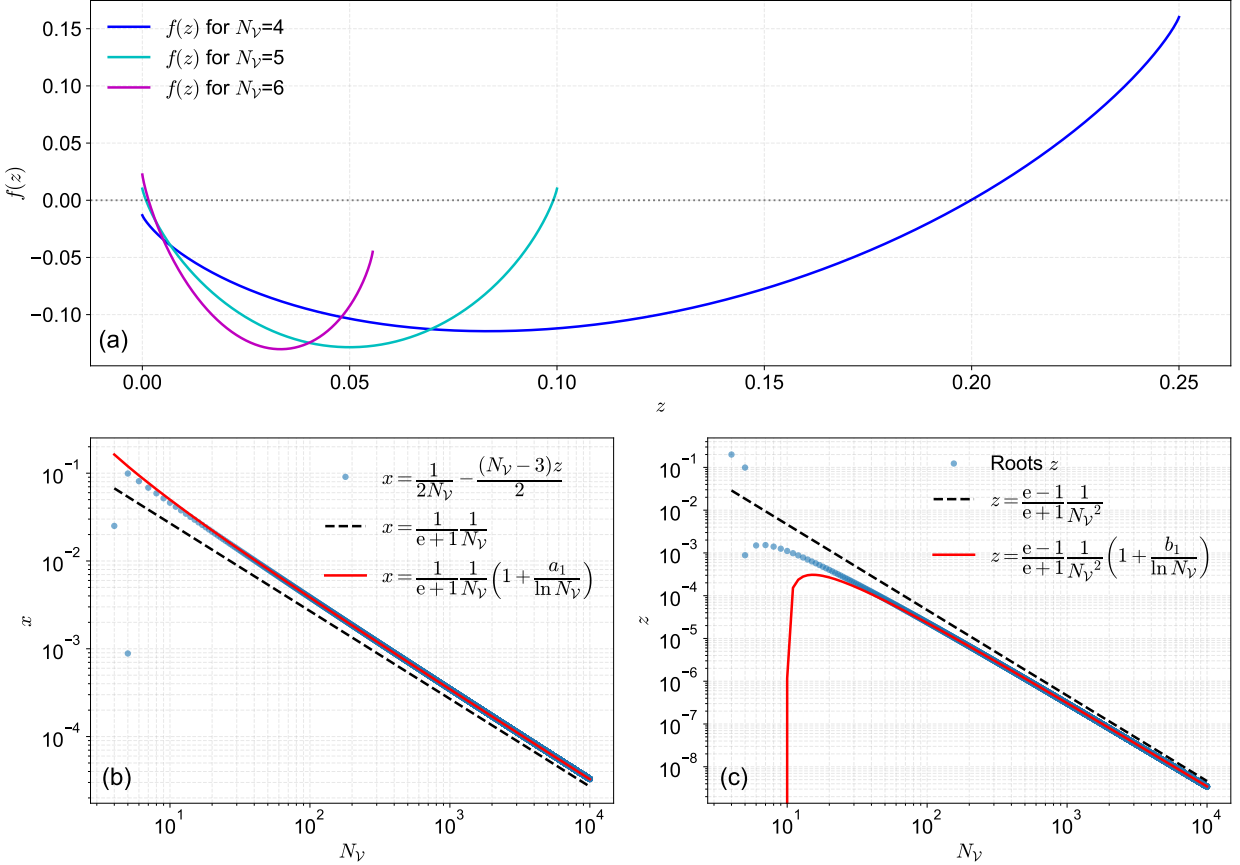


Fig. 4. The functions $f(z)$ for $N_V = 4, 5, 6$ (a), the values of x (b), and z (c) for different N_V . The black dashed line denotes its first-order approximation and the red line denotes its second-order approximation, where a_1 and b_1 are shown in Eq. (43).

The entropy balance equation

$$2x \ln x + (N_V - 3)z \ln z = -\frac{2e}{e+1} \cdot \frac{\ln N_V}{N_V} \quad (39)$$

can then be recast in terms of A and B as

$$A \ln A + B \ln B - A \ln 2 - B \ln(N_V - 3) = \left(\frac{1-e}{e+1}\right) \ln N_V. \quad (40)$$

As $N_V \rightarrow \infty$, we make the asymptotic ansatz

$$A = A_0 + \frac{a_1}{\ln N_V} + o\left(\frac{1}{\ln N_V}\right), \quad B = B_0 + \frac{b_1}{\ln N_V} + o\left(\frac{1}{\ln N_V}\right), \quad (41)$$

where A_0 and B_0 are the leading-order constants solving the $\ln N_V$ -independent balance:

$$A_0 + B_0 = 1, \quad A_0 = \frac{2}{e+1}, \quad B_0 = \frac{e-1}{e+1}. \quad (42)$$

Solving for the first-order logarithmic corrections gives

$$a_1 = \frac{1-e}{2}b_1, \quad b_1 = \ln(e-1) - \frac{e-1}{e+1}\ln(e+1), \quad (43)$$

thus leading to the following asymptotic expansions for x and z :

$$\begin{aligned} x &= \frac{A}{2N_V} = \frac{1}{e+1} \cdot \frac{1}{N_V} \left[1 + \frac{a_1}{\ln N_V} + O\left(\frac{1}{(\ln N_V)^2}\right) \right], \\ z &= \frac{B}{N_V(N_V-3)} = \frac{e-1}{e+1} \cdot \frac{1}{N_V^2} \left[1 + \frac{b_1}{\ln N_V} + O\left(\frac{1}{(\ln N_V)^2}\right) \right]. \end{aligned} \quad (44)$$

This result explains why, despite the apparent power-law decay of z , the quantity x scales linearly with N_V^{-1} , appearing as a straight line with slope -1 in a log-log plot. The logarithmic correction enters only at subleading order and becomes numerically negligible for moderate values of N_V , accounting for the agreement between theory and numerical solutions observed in Figs. 4(b-c). Hence, when $x = y$, the link weights x , y , and z that make the network resilience optimal exhibit a power law distribution as N_V is large.

3.3. The case of $y = z$

3.3.1. Existence of solutions

Assume $y = z$. Then Eqs. (23) reduce to

$$\begin{cases} x + (N_V - 2)z = \frac{1}{N_V}, \\ x \ln x + (N_V - 2)z \ln z = -\frac{2e}{e+1} \cdot \frac{\ln N_V}{N_V}, \end{cases} \quad (45)$$

where $x, z \geq 0$. The normalization condition yields

$$x = \frac{1}{N_V} - (N_V - 2)z. \quad (46)$$

Substituting this expression into the second equation gives

$$(N_V - 2)z \ln z + \left[\frac{1}{N_V} - (N_V - 2)z \right] \ln \left[\frac{1}{N_V} - (N_V - 2)z \right] = -\frac{2e}{e+1} \cdot \frac{\ln N_V}{N_V}. \quad (47)$$

The feasibility condition requires

$$0 \leq z \leq \frac{1}{N_V(N_V - 2)}. \quad (48)$$

To analyze the solution properties of Eq. (47), define

$$f(z) = (N_V - 2)z \ln z + \left[\frac{1}{N_V} - (N_V - 2)z \right] \ln \left[\frac{1}{N_V} - (N_V - 2)z \right] + \frac{2e}{e+1} \cdot \frac{\ln N_V}{N_V}. \quad (49)$$

Let $b = N_V - 2$ (with $b > 1$) and define

$$v(z) = \frac{1}{N_V} - bz. \quad (50)$$

Then

$$f(z) = bz \ln z + v(z) \ln v(z) + \frac{2e}{e+1} \cdot \frac{\ln N_V}{N_V}. \quad (51)$$

The first derivative of $f(z)$ is

$$\begin{aligned} f'(z) &= b(\ln z + 1) + v'(z)(\ln v(z) + 1) \\ &= b(\ln z + 1) - b(\ln v(z) + 1) \\ &= b \ln \left(\frac{z}{v(z)} \right). \end{aligned} \quad (52)$$

Hence, $f(z)$ is monotonically decreasing when $0 < z < \frac{1}{N_V(N_V - 1)}$ and monotonically increasing when $\frac{1}{N_V(N_V - 1)} < z < \frac{1}{N_V(N_V - 2)}$. The minimum value is attained at

$$z = \frac{1}{N_V(N_V - 1)}, \quad (53)$$

with

$$f(z)_{\min} = \frac{1}{N_V} \left(\frac{e-1}{e+1} \ln N_V - \ln(N_V - 1) \right). \quad (54)$$

For $N_V > 3$, $f(z)_{\min} < 0$.

The second derivative is

$$f''(z) = b \left(\frac{1}{z} + \frac{b}{v(z)} \right), \quad (55)$$

which is non-negative on the feasible domain, indicating that $f(z)$ is convex.

At the boundary points, we have

$$f(0) = -\frac{1}{N_V} \ln N_V + \frac{2e}{e+1} \cdot \frac{\ln N_V}{N_V} \quad (56)$$

and

$$f\left(\frac{1}{N_V(N_V-2)}\right) = -\frac{1}{N_V} \ln [N_V(N_V-2)] + \frac{2e}{e+1} \cdot \frac{\ln N_V}{N_V}. \quad (57)$$

Combining the convexity of $f(z)$ and the boundary values, we conclude that: when $N_V \geq 4$, we have $f(0) > 0$ and $f\left(\frac{1}{N_V(N_V-2)}\right) < 0$, thus Eq. (47) has a unique solution. This result reveals the existence of solutions of the optimal resilience when $y = z$.

3.3.2. Asymptotic behavior of solutions

Furthermore, by numerically solving $f(z) = 0$ for increasing N_V , we observe that when N_V becomes sufficiently large (e.g., $N_V > 10^2$), the relationship between N_V and the corresponding root z forms an approximately straight line in the double-logarithmic coordinate system, which suggests a power-law scaling. To describe the asymptotic behavior of the root pair (x, z) for large network size N_V , we introduce scaled variables

$$A = N_V x, \quad B = (N_V - 2) N_V z, \quad (58)$$

such that Eq. (46) is equivalent to

$$A + B = 1. \quad (59)$$

The entropy balance equation

$$x \ln x + (N_V - 2)z \ln z = -\frac{2e}{e+1} \cdot \frac{\ln N_V}{N_V} \quad (60)$$

can then be recast in terms of A and B as

$$A \ln A + B \ln B - B \ln(N_V - 2) = \left(\frac{1-e}{e+1} \right) \ln N_V. \quad (61)$$

As $N_V \rightarrow \infty$, we make the asymptotic ansatz

$$A = A_0 + \frac{a_1}{\ln N_V} + o\left(\frac{1}{\ln N_V}\right), \quad B = B_0 + \frac{b_1}{\ln N_V} + o\left(\frac{1}{\ln N_V}\right), \quad (62)$$

where A_0 and B_0 are the leading-order constants solving the $\ln N_V$ -independent balance:

$$A_0 + B_0 = 1, \quad A_0 = \frac{2}{e+1}, \quad B_0 = \frac{e-1}{e+1}. \quad (63)$$

Solving for the first-order logarithmic corrections gives

$$a_1 = \frac{1-e}{2}b_1, \quad b_1 = \ln(e-1) + \frac{2 \ln 2}{e-1} - \frac{e+1}{e-1} \ln(e+1), \quad (64)$$

thus leading to the following asymptotic expansions for x and z :

$$\begin{aligned} x &= \frac{A}{N_V} = \frac{2}{e+1} \cdot \frac{1}{N_V} \left[1 + \frac{a_1}{\ln N_V} + O\left(\frac{1}{(\ln N_V)^2}\right) \right], \\ z &= \frac{B}{N_V(N_V - 2)} = \frac{e-1}{e+1} \cdot \frac{1}{N_V^2} \left[1 + \frac{b_1}{\ln N_V} + O\left(\frac{1}{(\ln N_V)^2}\right) \right]. \end{aligned} \quad (65)$$

This result is similar to the result when $x = y$, where the quantity x remains tightly constrained to a straight line with slope -1 in the double-logarithmic representation. The logarithmic correction enters only at subleading order and becomes numerically negligible for moderate values of N_V , accounting for the agreement between theory and numerical solutions observed in Figs. 5(a-b). Hence, when $y = z$, the link weights x , y , and z that make the network resilience optimal exhibit

a power law distribution as N_V is large.

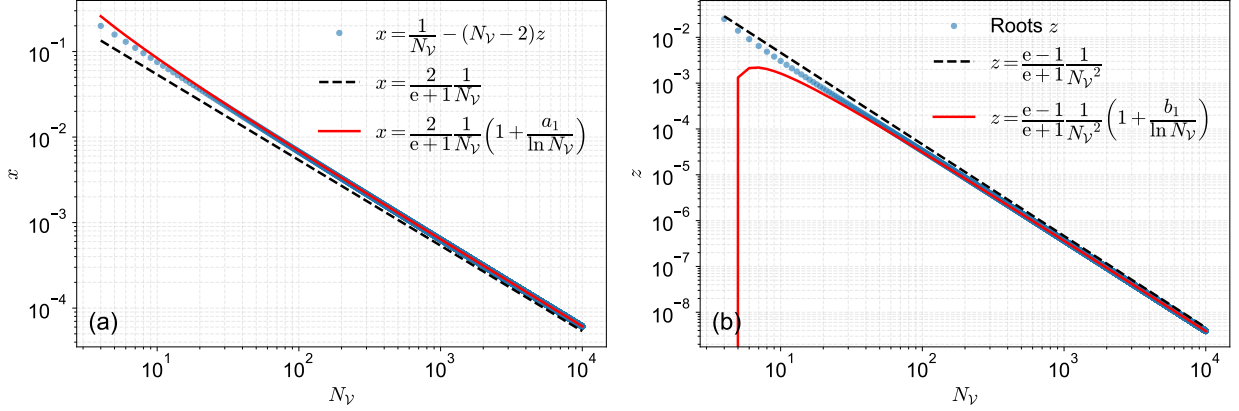


Fig. 5. The values of x (a) and z (b) for different N_V . The black dashed line denotes its first-order approximation and the red line denotes its second-order approximation, where a_1 and b_1 are shown in Eq. (64).

3.3.3. Existence of the optimal resilience

Here we employ the case of $y = z$ to prove the universality of the optimal resilience in complex networks and thereby propose two theorems.

Theorem 1. *Let $N_V \geq 3$ and $\mathcal{V} = \{1, \dots, N_V\}$. In the set of all feasible network configurations*

$$\mathcal{P} = \left\{ \mathbf{p} = (p_{ij})_{i,j=1}^{N_V} : p_{ij} \geq 0, p_{ii} = 0, \sum_{i=1}^{N_V} \sum_{j=1}^{N_V} p_{ij} = 1 \right\}, \quad (66)$$

there exists at least an optimal configuration $\mathbf{p}^ \in \mathcal{P}$ such that*

$$\alpha(\mathbf{p}^*) = \frac{e(\mathbf{p}^*)}{e(\mathbf{p}^*) + r(\mathbf{p}^*)} = \frac{1}{e}, \quad (67)$$

and hence the resilience attains its optimal value:

$$R(\mathbf{p}^*) = -\alpha(\mathbf{p}^*) \ln \alpha(\mathbf{p}^*) = \frac{1}{e}. \quad (68)$$

Proof. The set \mathcal{P} is a closed and bounded convex subset of $\mathbb{R}^{N_V(N_V-1)}$, and hence compact. Rewrite

the marginal distributions

$$p_i^{\text{out}} = \sum_{j=1}^{N_V} p_{ij}, \quad p_j^{\text{in}} = \sum_{i=1}^{N_V} p_{ij}. \quad (69)$$

Since the function $x \mapsto -x \ln x$ is continuous on $[0, 1]$ and the marginals are linear mappings of \mathbf{p} , both $e(\mathbf{p})$ and $r(\mathbf{p})$ are continuous on \mathcal{P} . Whenever $e(\mathbf{p}) + r(\mathbf{p}) > 0$, we have

$$\alpha(\mathbf{p}) = \frac{e(\mathbf{p})}{e(\mathbf{p}) + r(\mathbf{p})} \in [0, 1], \quad (70)$$

thus α is continuous on \mathcal{P} (with continuous extension at the boundary).

Let us construct two uniformly distributed extreme network structures: a complete network and a unidirectional ring network, as shown in Fig. 6.

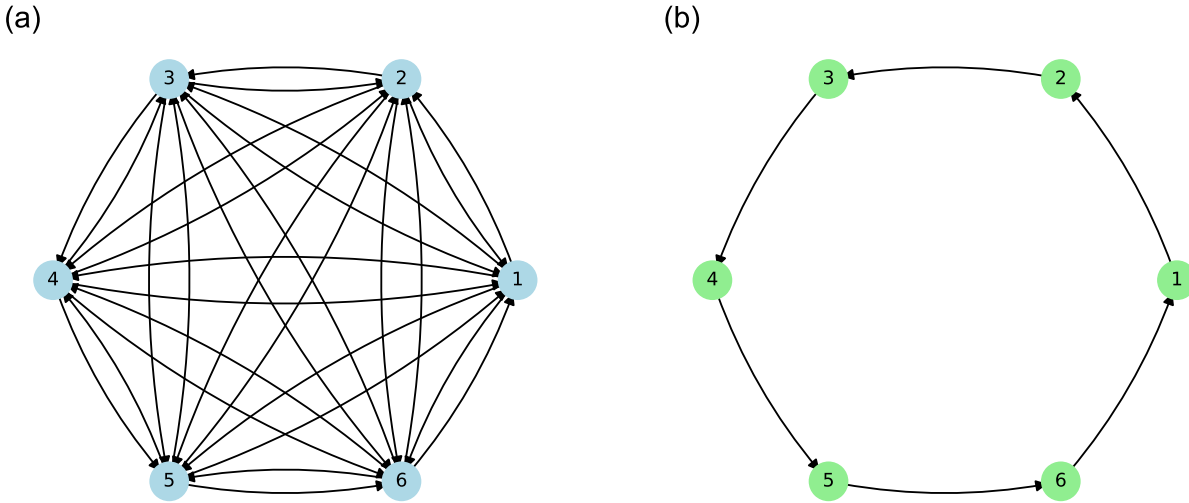


Fig. 6. Complete network (a) and unidirectional ring network (b).

(i) *Complete network.* Let $\bar{\mathbf{p}} = \{\bar{p}_{ij} : i, j = 1, \dots, N_V\}$, where

$$\bar{p}_{ij} = \begin{cases} \frac{1}{N_V(N_V - 1)}, & i \neq j, \\ 0, & i = j. \end{cases} \quad (71)$$

Then, we have

$$e(\bar{\mathbf{p}}) = \sum_{i=1}^{N_V} \sum_{j=1}^{N_V} \frac{1}{N_V(N_V-1)} \ln \frac{N_V(N_V-1)}{(N_V-1)^2} = \ln \frac{N_V}{N_V-1}, \quad (72)$$

$$r(\bar{\mathbf{p}}) = \sum_{i=1}^{N_V} \sum_{j=1}^{N_V} \frac{1}{N_V(N_V-1)} \ln(N_V-1)^2 = 2 \ln(N_V-1), \quad (73)$$

and

$$\alpha(\bar{\mathbf{p}}) = \frac{\ln N_V - \ln(N_V-1)}{\ln N_V + \ln(N_V-1)}, \quad (74)$$

where $\alpha(\bar{\mathbf{p}}) < 1/e$ for $N_V \geq 3$.

(ii) *Unidirectional ring network.* Let $\tilde{\mathbf{p}} = \{\tilde{p}_{ij} : i, j = 1, \dots, N_V\}$, where

$$\tilde{p}_{ij} = \begin{cases} \frac{1}{N_V}, & j = \text{mod}(i+1, N_V), \\ 0, & \text{otherwise.} \end{cases} \quad (75)$$

Then, we have

$$e(\tilde{\mathbf{p}}) = \sum_{i=1}^{N_V} \sum_{j=1}^{N_V} \frac{1}{N_V} \ln \frac{N_V^2}{N_V} = \ln N_V, \quad (76)$$

$$r(\tilde{\mathbf{p}}) = \sum_{i=1}^{N_V} \sum_{j=1}^{N_V} \frac{1}{N_V} \ln \frac{N_V^2}{N_V^2} = 0, \quad (77)$$

and

$$\alpha(\tilde{\mathbf{p}}) = 1, \quad (78)$$

indicating this network is overly-efficient and possesses deterministic structure.

Since \mathcal{P} is convex, for any $\lambda \in [0, 1]$, let

$$\mathbf{p}(\lambda) = (1-\lambda)\bar{\mathbf{p}} + \lambda\tilde{\mathbf{p}} \in \mathcal{P}. \quad (79)$$

The function $\alpha(\mathbf{p}(\lambda))$ of λ is continuous on $[0, 1]$ and satisfies

$$\alpha(\mathbf{p}(0)) = \alpha(\bar{\mathbf{p}}) < \frac{1}{e}, \quad \alpha(\mathbf{p}(1)) = \alpha(\tilde{\mathbf{p}}) = 1 > \frac{1}{e}. \quad (80)$$

By the intermediate value theorem, there exists $\lambda^* \in (0, 1)$ such that

$$\alpha(\mathbf{p}(\lambda^*)) = \frac{1}{e}. \quad (81)$$

Setting $\mathbf{p}^* = \mathbf{p}(\lambda^*)$ completes the proof. Consequently, for networks with at least three nodes, there exists at least a joint distribution such that resilience is optimized ($R = 1/e$). \square

The resulting joint probabilities of Theorem 1 are given by

$$p_{ij}(\lambda) = \begin{cases} \frac{1 + \lambda(N_V - 2)}{N_V(N_V - 1)}, & j = \text{mod}(i + 1, N_V), \\ \frac{1 - \lambda}{N_V(N_V - 1)}, & j \neq i, \text{ mod}(i + 1, N_V), \\ 0, & i = j. \end{cases} \quad (82)$$

For all $\lambda \in [0, 1]$, the marginal distributions remain uniform:

$$p_i^{\text{out}}(\lambda) = \frac{1}{N_V}, \quad p_j^{\text{in}}(\lambda) = \frac{1}{N_V}, \quad \forall i, j. \quad (83)$$

Hence, variations in λ affect only the joint structure of flows, while the marginals retain maximal entropy.

Theorem 2. *Let $N_V \geq 3$ and $N_V = \{1, \dots, N_V\}$. In the set of all feasible network configurations \mathcal{P} expressed as Eq. (66), if the marginal distributions remain uniform:*

$$p_i^{\text{out}} = p_j^{\text{in}} = \frac{1}{N_V}, \quad (84)$$

there always exist the following equations:

$$r = 2 \ln N_V - 2e \quad (85)$$

and

$$\alpha = \frac{e}{2 \ln N_V - e}, \quad (86)$$

and the optimal condition $\alpha = 1/e$ is equivalent to

$$e = \frac{2 \ln N_V}{e + 1}. \quad (87)$$

Proof. When $p_i^{\text{out}} = p_j^{\text{in}} = \frac{1}{N_V}$, we have

$$\begin{aligned} r &= - \sum_{i=1}^{N_V} \sum_{j=1}^{N_V} p_{ij} \ln \left(\frac{p_{ij}}{p_i^{\text{out}}} \right) - \sum_{i=1}^{N_V} \sum_{j=1}^{N_V} p_{ij} \ln \left(\frac{p_{ij}}{p_j^{\text{in}}} \right) \\ &= -2 \sum_{i=1}^{N_V} \sum_{j=1}^{N_V} p_{ij} \ln (N_V p_{ij}) \\ &= -2 \ln N_V + 2H \\ &= 2 \ln N_V - 2e. \end{aligned} \quad (88)$$

Consequently, the order parameter α takes the closed form

$$\alpha = \frac{e}{e + r} = \frac{e}{2 \ln N_V - e}. \quad (89)$$

The optimal condition $\alpha = 1/e$ is equivalent to

$$e = \frac{2 \ln N_V}{e + 1}. \quad (90)$$

□

According to Theorem 2, for the joint probabilities given by Eq. (82), we have

$$\begin{aligned}
e(\lambda) &= \sum_{i=1}^{N_V} \sum_{j=1}^{N_V} p_{ij}(\lambda) \ln \left(\frac{p_{ij}(\lambda)}{p_i^{\text{out}} p_j^{\text{in}}} \right) \\
&= \sum_{i=1}^{N_V} \sum_{j=1}^{N_V} p_{ij}(\lambda) \ln (N_V^2 p_{ij}(\lambda)) \\
&= \frac{1 + \lambda(N_V - 2)}{N_V - 1} \ln \left(\frac{N_V(1 + \lambda(N_V - 2))}{N_V - 1} \right) + \frac{(N_V - 2)(1 - \lambda)}{N_V - 1} \ln \left(\frac{N_V(1 - \lambda)}{N_V - 1} \right)
\end{aligned} \tag{91}$$

and

$$\begin{aligned}
r(\lambda) &= - \sum_{i=1}^{N_V} \sum_{j=1}^{N_V} p_{ij}(\lambda) \ln \left(\frac{p_{ij}(\lambda)}{p_i^{\text{out}}} \right) - \sum_{i=1}^{N_V} \sum_{j=1}^{N_V} p_{ij}(\lambda) \ln \left(\frac{p_{ij}(\lambda)}{p_j^{\text{in}}} \right) \\
&= -2 \sum_{i=1}^{N_V} \sum_{j=1}^{N_V} p_{ij}(\lambda) \ln (N_V p_{ij}(\lambda)) \\
&= 2 \ln N_V - 2e(\lambda).
\end{aligned} \tag{92}$$

Consequently, the order parameter $\alpha(\lambda)$ takes the closed form

$$\alpha(\lambda) = \frac{e(\lambda)}{e(\lambda) + r(\lambda)} = \frac{e(\lambda)}{2 \ln N_V - e(\lambda)}. \tag{93}$$

The optimal condition $\alpha(\lambda^*) = 1/e$ is equivalent to

$$e(\lambda^*) = \frac{2 \ln N_V}{e + 1}. \tag{94}$$

Substituting the explicit expression of $e(\lambda^*)$ yields the following scalar equation for λ^* :

$$\frac{1 + \lambda^*(N_V - 2)}{N_V - 1} \ln \left(\frac{N_V(1 + \lambda^*(N_V - 2))}{N_V - 1} \right) + \frac{(N_V - 2)(1 - \lambda^*)}{N_V - 1} \ln \left(\frac{N_V(1 - \lambda^*)}{N_V - 1} \right) = \frac{2 \ln N_V}{e + 1}, \tag{95}$$

which has a unique solution $\lambda^* \in (0, 1)$ for any $N_V \geq 3$. When $N_V = 7$, λ^* reaches its maximum value (0.728). When $N_V \rightarrow +\infty$, λ^* converges to $\frac{2}{e + 1} > 0.5$, as shown in Fig. 7. Consequently, for the interpolated family between a complete directed graph and a deterministic ring, the optimal configuration has an explicit characterization through a one-dimensional equation. The results

reveal that the more nodes there are, the more the interpolating family needs to be biased towards efficient structures to achieve the optimal resilience.

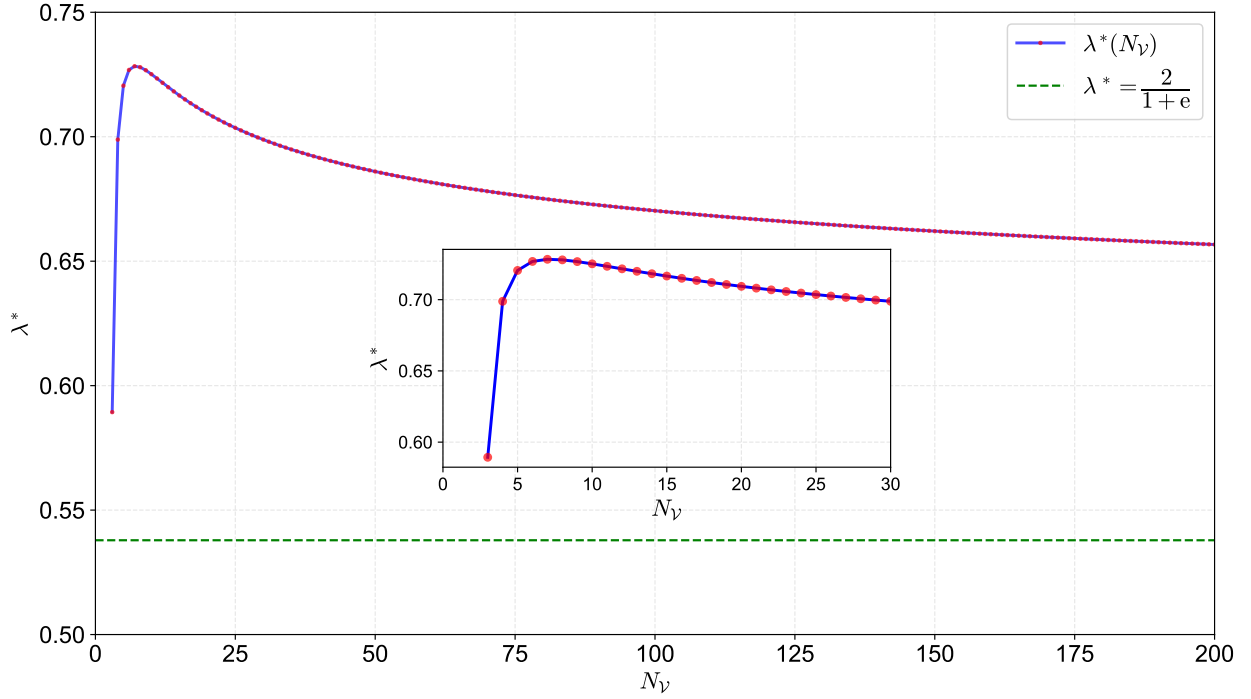


Fig. 7. The relationship between N_V and the parameter of the optimal condition λ^* .

3.4. The case of $z = 0$

Assume $z = 0$. Eqs. (23) reduce to

$$\begin{cases} x + y = \frac{1}{N_V}, \\ x \ln x + y \ln y = -\frac{2e}{e+1} \cdot \frac{\ln N_V}{N_V}, \end{cases} \quad (96)$$

where $x, y \geq 0$. The normalization condition yields

$$y = \frac{1}{N_V} - x. \quad (97)$$

Substituting this expression into the second equation gives

$$x \ln x + \left(\frac{1}{N_V} - x \right) \ln \left(\frac{1}{N_V} - x \right) = -\frac{2e}{e+1} \cdot \frac{\ln N_V}{N_V}. \quad (98)$$

The feasible condition requires

$$0 \leq x \leq \frac{1}{N_V}. \quad (99)$$

To analyze the solution structure of Eq. (98), define

$$f(x) = x \ln x + \left(\frac{1}{N_V} - x \right) \ln \left(\frac{1}{N_V} - x \right) + \frac{2e}{e+1} \cdot \frac{\ln N_V}{N_V}. \quad (100)$$

The first derivative of $f(x)$ is

$$\begin{aligned} f'(x) &= \ln x + 1 - \left[\ln \left(\frac{1}{N_V} - x \right) + 1 \right] \\ &= \ln \left(\frac{x}{\frac{1}{N_V} - x} \right). \end{aligned} \quad (101)$$

Hence, $f(x)$ is monotonically decreasing when $0 < x < \frac{1}{2N_V}$ and monotonically increasing when $\frac{1}{2N_V} < x < \frac{1}{N_V}$. The minimum value is attained at

$$x = \frac{1}{2N_V} \quad (102)$$

with

$$f(x)_{\min} = \frac{1}{N_V} \left[\frac{e-1}{e+1} \ln N_V - \ln 2 \right]. \quad (103)$$

For $N_V = 4$, $f(x)_{\min} < 0$, and $N_V > 4$, $f(x)_{\min} > 0$.

The second derivative is

$$f''(x) = \frac{1}{x} + \frac{1}{\frac{1}{N_V} - x}, \quad (104)$$

which is non-negative on the feasible domain, indicating that $f(x)$ is convex.

At the boundary points, we have

$$f(0) = f\left(\frac{1}{N_V}\right) = \frac{e-1}{e+1} \cdot \frac{\ln N_V}{N_V}. \quad (105)$$

Combining the convexity of $f(x)$ and the boundary values, we conclude that: (1) when $N_V = 4$, we have $f(x)_{\min} < 0$ and $f(0) = f\left(\frac{1}{N_V}\right) \geq 0$, thus Eq. (98) has two solutions; and (2) when $N_V > 4$, we have $f(x)_{\min} > 0$ and $f(0) = f\left(\frac{1}{N_V}\right) \geq 0$, thus Eq. (98) has no solution. The above situations are illustrated in Fig. 8, which reveals that there exists no optimal resilience for networks with more than four nodes when $z = 0$.

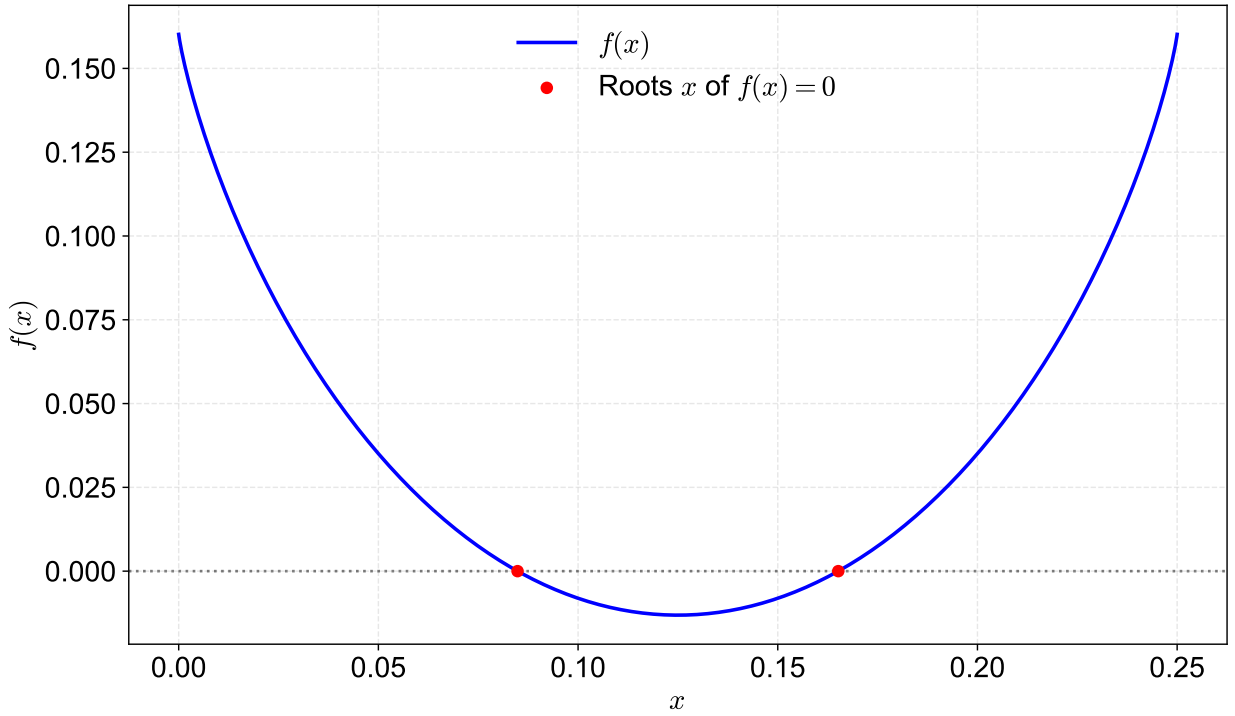


Fig. 8. The function $f(x)$ and roots x for $N_V = 4$.

3.5. The case of $y = 0$

3.5.1. Existence of solutions

Assume $y = 0$. Then Eqs. (23) reduce to

$$\begin{cases} x + (N_V - 3)z = \frac{1}{N_V}, \\ x \ln x + (N_V - 3)z \ln z = -\frac{2e}{e+1} \cdot \frac{\ln N_V}{N_V}, \end{cases} \quad (106)$$

where $x, z \geq 0$. The normalization condition yields

$$x = \frac{1}{N_V} - (N_V - 3)z. \quad (107)$$

Substituting this expression into the second equation gives

$$\left[\frac{1}{N_V} - (N_V - 3)z \right] \ln \left[\frac{1}{N_V} - (N_V - 3)z \right] + (N_V - 3)z \ln z = -\frac{2e}{e+1} \cdot \frac{\ln N_V}{N_V}. \quad (108)$$

The feasible condition requires

$$0 \leq z \leq \frac{1}{N_V(N_V - 3)}. \quad (109)$$

To analyze the solution properties of Eq. (108), define

$$f(z) = \left[\frac{1}{N_V} - (N_V - 3)z \right] \ln \left[\frac{1}{N_V} - (N_V - 3)z \right] + (N_V - 3)z \ln z + \frac{2e}{e+1} \cdot \frac{\ln N_V}{N_V}. \quad (110)$$

Let $a = N_V - 3 > 0$ and define

$$u(z) = \frac{1}{N_V} - az. \quad (111)$$

Then $f(z)$ can be written as

$$f(z) = u(z) \ln u(z) + az \ln z + \frac{2e}{e+1} \cdot \frac{\ln N_V}{N_V}. \quad (112)$$

The first derivative of $f(z)$ is

$$\begin{aligned}
f'(z) &= u'(z) \ln u(z) + u'(z) + a(\ln z + 1) \\
&= -a[\ln u(z) + 1] + a(\ln z + 1) \\
&= a \ln \left(\frac{z}{u(z)} \right).
\end{aligned} \tag{113}$$

Hence, $f(z)$ is monotonically decreasing when $0 < z < \frac{1}{N_V(N_V - 2)}$ and monotonically increasing when $\frac{1}{N_V(N_V - 2)} < z < \frac{1}{N_V(N_V - 3)}$. The minimum value is attained at

$$z = \frac{1}{N_V(N_V - 2)} \tag{114}$$

with

$$f(z)_{\min} = \frac{1}{N_V} \left(\frac{e-1}{e+1} \ln N_V - \ln(N_V - 2) \right). \tag{115}$$

For $N_V > 3$, $f(z)_{\min} < 0$.

The second derivative is

$$f''(z) = \frac{a}{z} + \frac{a^2}{u(z)}, \tag{116}$$

which is non-negative on the feasible domain, indicating that $f(z)$ is convex.

At the boundary points, we have

$$f(0) = -\frac{1}{N_V} \ln N_V + \frac{2e}{e+1} \cdot \frac{\ln N_V}{N_V} = \frac{e-1}{e+1} \cdot \frac{\ln N_V}{N_V} \tag{117}$$

and

$$f\left(\frac{1}{N_V(N_V - 3)}\right) = -\frac{1}{N_V} \ln [N_V(N_V - 3)] + \frac{2e}{e+1} \cdot \frac{\ln N_V}{N_V}. \tag{118}$$

Combining the convexity of $f(x)$ and the boundary values, we conclude that: (1) when $4 \leq N_V \leq 5$, we have $f(0) > 0$ and $f\left(\frac{1}{N_V(N_V - 3)}\right) > 0$, thus Eq. (108) has two solutions; and (2) when $N_V > 5$, we have $f(0) > 0$ and $f\left(\frac{1}{N_V(N_V - 3)}\right) < 0$, thus Eq. (108) has a unique solution. The above situations are illustrated in Fig. 9(a), which reveals the existence of solutions of the optimal

resilience when $y = 0$.

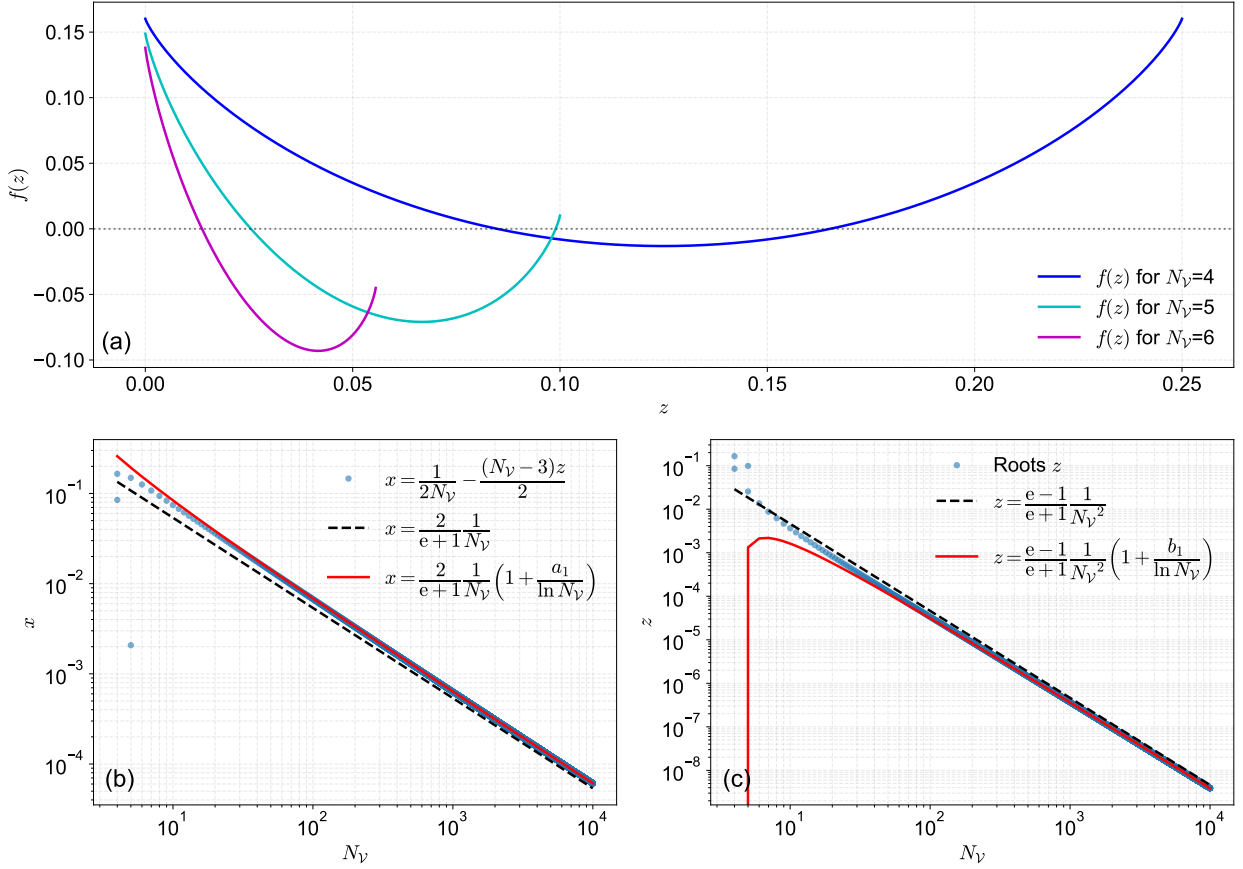


Fig. 9. The functions $f(z)$ for $N_V = 4, 5, 6$ (a), the values of x (b), and z (c) for different N_V . The black dashed line denotes its first-order approximation and the red line denotes its second-order approximation, where a_1 and b_1 are shown in Eq. (125).

3.5.2. Asymptotic behavior of solutions

Furthermore, by numerically solving $f(z) = 0$ for increasing N_V , we observe that when N_V becomes sufficiently large (e.g., $N_V > 10^2$), the relationship between N_V and the corresponding root z forms an approximately straight line in the double-logarithmic coordinate system, which suggests a power-law scaling. To describe the asymptotic behavior of the root pair (x, z) for large network size N_V , we introduce scaled variables

$$A = N_V x, \quad B = (N_V - 3) N_V z, \quad (119)$$

such that Eq. (107) is equivalent to

$$A + B = 1. \quad (120)$$

The entropy balance equation

$$x \ln x + (N_V - 3)z \ln z = -\frac{2e}{e+1} \cdot \frac{\ln N_V}{N_V} \quad (121)$$

can then be recast in terms of A and B as

$$A \ln A + B \ln B - B \ln(N_V - 3) = \left(\frac{1-e}{e+1} \right) \ln N_V. \quad (122)$$

As $N_V \rightarrow \infty$, we make the asymptotic ansatz

$$A = A_0 + \frac{a_1}{\ln N_V} + o\left(\frac{1}{\ln N_V}\right), \quad B = B_0 + \frac{b_1}{\ln N_V} + o\left(\frac{1}{\ln N_V}\right), \quad (123)$$

where A_0 and B_0 are the leading-order constants solving the $\ln N_V$ -independent balance:

$$A_0 + B_0 = 1, \quad A_0 = \frac{2}{e+1}, \quad B_0 = \frac{e-1}{e+1}. \quad (124)$$

Solving for the first-order logarithmic corrections gives

$$a_1 = \frac{1-e}{2}b_1, \quad b_1 = \ln(e-1) + \frac{2\ln 2}{e-1} - \frac{e+1}{e-1} \ln(e+1), \quad (125)$$

thus leading to the following asymptotic expansions for x and z :

$$\begin{aligned} x &= \frac{A}{N_V} = \frac{2}{e+1} \cdot \frac{1}{N_V} \left[1 + \frac{a_1}{\ln N_V} + O\left(\frac{1}{(\ln N_V)^2}\right) \right], \\ z &= \frac{B}{N_V(N_V - 3)} = \frac{e-1}{e+1} \cdot \frac{1}{N_V^2} \left[1 + \frac{b_1}{\ln N_V} + O\left(\frac{1}{(\ln N_V)^2}\right) \right]. \end{aligned} \quad (126)$$

This result is similar to the results when $x = y$ and $y = z$, where the quantity x remains tightly constrained to a straight line with slope -1 in the double-logarithmic representation. The logarithmic correction enters only at subleading order and becomes numerically negligible for

moderate values of N_V , accounting for the agreement between theory and numerical solutions observed in Figs. 9(b-c). Hence, when $y = 0$, the link weights x , y , and z that make the network resilience optimal exhibit a power law distribution as N_V is large.

4. Conclusion

This study provides a theoretical investigation of entropy-based resilience optimization in directed flow networks. By analyzing Ulanowicz's resilience metric within a constrained optimization framework, we establish the existence of optimal resilience configurations for networks with at least three nodes and demonstrate the structural impossibility of achieving the optimal state in two-node systems. These results clarify the fundamental role of network scale in enabling efficiency-redundancy trade off.

Using a symmetric multi-link network model, we derive explicit governing equations for optimal flow allocations and obtain closed-form asymptotic scaling laws for large networks. The analytical results show that dominant links scale inversely with network size, while background links exhibit quadratic decay with logarithmic corrections. This structural separation between primary and secondary flows reflects an intrinsic organizational principle of robust network design: high-throughput backbone connections coexist with sparse redundancy channels that collectively enhance system resilience.

From an operations research perspective, these findings offer quantitative guidance for designing large-scale networked systems under robustness constraints (Ambulkar et al., 2015). The entropy-based framework provides a tractable analytical tool for studying trade-offs between performance efficiency and structural redundancy, which are central concerns in supply chain management, transportation planning, and infrastructure design. Future research may extend this framework by incorporating capacity constraints, cost functions, stochastic demand, and dynamic adaptation mechanisms, thereby further bridging entropy-based resilience theory and practical network optimization problems.

Acknowledgment

This work was partly supported by the National Natural Science Foundation of China (72171083) and the Fundamental Research Funds for the Central Universities.

Declaration of competing interest

The authors declare that they have no known competing financial interests or personal relationships that could have appeared to influence the work reported in this paper.

Data availability

Data will be made available on request.

References

Ambulkar, S., Blackhurst, J., Grawe, S., 2015. Firm's resilience to supply chain disruptions: scale development and empirical examination. *Journal of Operations Management* 33-34, 111–122. doi:[10.1016/j.jom.2014.11.002](https://doi.org/10.1016/j.jom.2014.11.002).

Brunnermeier, M.K., 2024. Presidential address: Macrofinance and resilience. *Journal of Finance* 79, 3683–3728. doi:[10.1111/jofi.13403](https://doi.org/10.1111/jofi.13403).

Chen, X., Ma, S., Chen, L., Yang, L., 2024. Resilience measurement and analysis of intercity public transportation network. *Transportation Research Part D* 131, 104202. doi:[10.1016/j.trd.2024.104202](https://doi.org/10.1016/j.trd.2024.104202).

Cohen, M., Cui, S., Doetsch, S., Ernst, R., Huchzermeier, A., Kouvelis, P., Lee, H., Matsuo, H., Tsay, A.A., 2022. Bespoke supply-chain resilience: the gap between theory and practice. *Journal of Operations Management* 68, 515–531. doi:[10.1002/joom.1184](https://doi.org/10.1002/joom.1184).

Goerner, S.J., Lietaer, B., Ulanowicz, R.E., 2009. Quantifying economic sustainability: Implications for free-enterprise theory, policy and practice. *Ecological Economics* 69, 76–81. doi:[10.1016/j.ecolecon.2009.07.018](https://doi.org/10.1016/j.ecolecon.2009.07.018).

Ivanov, D., 2024. Supply chain resilience: conceptual and formal models drawing from immune system analogy. *Omega-International Journal of Management Science* 127, 103081. doi:[10.1016/j.omega.2024.103081](https://doi.org/10.1016/j.omega.2024.103081).

Kahiluoto, H., Mäkinen, H., Kaseva, J., 2020. Supplying resilience through assessing diversity of responses to disruption. *International Journal of Operations & Production Management* 40, 271–292. doi:[10.1108/IJOPM-01-2019-0006](https://doi.org/10.1108/IJOPM-01-2019-0006).

Khakifirooz, M., Fathi, M., Dolgui, A., Pardalos, P.M., 2025. Assessing resiliency in scale-free supply chain networks: a stress testing approach based on entropy measurements and value-at-risk analysis. *International Journal of Production Research* 63, 3331–3364. doi:[10.1080/00207543.2024.2361850](https://doi.org/10.1080/00207543.2024.2361850).

Kharrazi, A., Rovenskaya, E., Fath, B.D., 2017. Network structure impacts global commodity trade growth and resilience. *PLoS One* 12, e0171184. doi:[10.1371/journal.pone.0171184](https://doi.org/10.1371/journal.pone.0171184).

Kharrazi, A., Rovenskaya, E., Fath, B.D., Yarime, M., Kraines, S., 2013. Quantifying the sustainability of economic resource networks: An ecological information-based approach. *Ecological Economics* 90, 177–186. doi:[10.1016/j.ecolecon.2013.03.018](https://doi.org/10.1016/j.ecolecon.2013.03.018).

Liang, S., Yu, Y., Kharrazi, A., Fath, B.D., Feng, C., Daigger, G.T., Chen, S., Ma, T., Zhu, B., Mi, Z., Yang, Z., 2020. Network resilience of phosphorus cycling in China has shifted by natural flows, fertilizer use and dietary transitions between 1600 and 2012. *Nature Food* 1, 365–375. doi:[10.1038/s43016-020-0098-6](https://doi.org/10.1038/s43016-020-0098-6).

Liu, X., Li, D., Ma, M., Szymanski, B.K., Stanley, H.E., Gao, J., 2022. Network resilience. *Physics Reports* 971, 1–108. doi:[10.1016/j.physrep.2022.04.002](https://doi.org/10.1016/j.physrep.2022.04.002).

Lücker, F., Timonina-Farkas, A., Seifert, R.W., 2025. Balancing resilience and efficiency: a literature review on overcoming supply chain disruptions. *Production and Operations Management* 34, 1495–1511. doi:[10.1177/10591478241302735](https://doi.org/10.1177/10591478241302735).

Luo, Z., Yu, Y., Kharrazi, A., Fath, B.D., Matsubae, K., Liang, S., Chen, D., Zhu, B., Ma, T., Hu, S., 2024. Decreasing resilience of China's coupled nitrogen-phosphorus cycling network requires urgent action. *Nature Food* 5, 48–58. doi:[10.1038/s43016-023-00889-5](https://doi.org/10.1038/s43016-023-00889-5).

Pettit, T.J., Croxton, K.L., Fiksel, J., 2019. The evolution of resilience in supply chain management: a retrospective on ensuring supply chain resilience. *Journal of Business Logistics* 40, 56–65. doi:[10.1111/jbl.12202](https://doi.org/10.1111/jbl.12202).

Reggiani, A., 2022. The architecture of connectivity: a key to network vulnerability, complexity and resilience. *Networks & Spatial Economics* 22, 415–437. doi:[10.1007/s11067-022-09563-y](https://doi.org/10.1007/s11067-022-09563-y).

Rutledge, R.W., Basore, B.L., Mulholland, R.J., 1976. Ecological stability: An information theory viewpoint. *Journal of Theoretical Biology* 57, 355–371. doi:[10.1016/0022-5193\(76\)90007-2](https://doi.org/10.1016/0022-5193(76)90007-2).

Seidl, R., Spies, T.A., Peterson, D.L., Stephens, S.L., Hicke, J.A., 2016. Searching for resilience: addressing the impacts of changing disturbance regimes on forest ecosystem services. *Journal of Applied Ecology* 53, 120–129. doi:[10.1111/1365-2664.12511](https://doi.org/10.1111/1365-2664.12511).

Ulanowicz, R.E., 1979. Complexity, stability and self-organization in natural communities. *Oecologia* 43, 295–298. doi:[10.1007/BF00344956](https://doi.org/10.1007/BF00344956).

Ulanowicz, R.E., 2009. The dual nature of ecosystem dynamics. *Ecological Modelling* 220, 1886–1892. doi:[10.1016/j.ecolmodel.2009.04.015](https://doi.org/10.1016/j.ecolmodel.2009.04.015).

Ulanowicz, R.E., Goerner, S.J., Lietaer, B., Gomez, R., 2009. Quantifying sustainability: Resilience, efficiency and the return of information theory. *Ecological Complexity* 6, 27–36. doi:[10.1016/j.ecocom.2008.10.005](https://doi.org/10.1016/j.ecocom.2008.10.005).

Ulanowicz, R.E., Norden, J.S., 1990. Symmetrical overhead in flow networks. *International Journal of Systems Science* 21, 429–437. doi:[10.1080/00207729008910372](https://doi.org/10.1080/00207729008910372).

Yang, Z., Wu, M., Sun, J., Zhang, Y., 2024. Aligning redundancy and flexibility for supply chain resilience: a literature synthesis. *Journal of Risk Research* 27, 313–335. doi:[10.1080/13669877.2024.2328196](https://doi.org/10.1080/13669877.2024.2328196).

Zhu, Y., Bao, Y., Qin, L., Sun, Q., Shia, B.C., Chen, M.C., 2025. Resilience analysis based on multi-layer network community detection of supply chain network. *Annals of Operations Research* doi:[10.1007/s10479-024-06426-2](https://doi.org/10.1007/s10479-024-06426-2).

Zorach, A.C., Ulanowicz, R.E., 2003. Quantifying the complexity of flow networks: How many roles are there? *Complexity* 8, 68–76. doi:[10.1002/cplx.10075](https://doi.org/10.1002/cplx.10075).